Electronic Supplementary Material (ESI) for Journal of Materials Chemistry A.

Supplementary Information

Robust and Superhydrophobic Thiourethane Bridged Polysilsesquioxane Aerogels as A Potential Thermal Insulation Material

Fangxin Zou,[a] Peng Yue,[b] Xinghua Zheng,[b] Dawei Tang,[b] Wenxin Fu*[a] and Zhibo Li*[c]

[a]*Beijing National Laboratory of Molecular Sciences (BNLMS), Institute of Chemistry, Chinese Academy of Sciences, Beijing 100190, P.R. China, *E-mail: fuwenxin@iccas.ac.cn*

[b]*Institute of Engineering Thermophysics, Chinese Academy of Sciences, Beijing 100090, P.R. China.*

[c]*School of Polymer Science and Engineering, Qingdao University of Science and Technology, Qingdao 266042, P.R. China, E-mail: zbli@qust.edu.cn*

Experimental

Materials:

Hexamethlene diisocyanate (HDI), Methylene diphenyl diisocyanate (MDI) and dicyclohexylmethylmethane-4, 4-diisocyanate (H_{12}MDI) were purchased from Aladin. (3-Mercaptopropyl) trimethoxysilane (MPTMS) was purchased from Beijing HWRK Chem Co. Ltd. Ethanol, tetrahydrofuran, n-heptane, hydrochloric acid (37wt% aqueous solution) and triethylamine (TEA) were purchased from Sinopharm Chemical Reagent Beijing Co. All the reagents were used as received without any further purification.

Synthesis:

General procedure for the synthesis of thiourethane bridged silsesquioxane precursors

Three kinds of thiourethane bridged silsesqiuoxane precursors are designated as HDI-BSQ, H_{12}MDI-BSQ and MDI-BSQ. HDI-BSQ, H_{12}MDI-BSQ and MDI-BSQ represent the precursors obtained from the click reaction of MPTMS with HDI, H_{12}MDI and MDI, respectively (Figure 1). For the thiol-isocyanate click reaction, a certain amount of MPTMS, diisocyanate and tetrahydrofuran were put into a round-bottom flask, and then TEA (1.7 wt% of total reactants amount, while the mass percent was 12% for the synthesis of H_{12}MDI-BSQ) as the catalyst was added into the mixture under stirring. The final molar ratio of SH/ NCO was 1 and the final reaction concentration of MPTMS was 0.8mol L^{-1}. Then the reaction was continued for another 12h at room temperature. The completion of the thiol-isocyanate reaction was monitored by FTIR, demonstrated by the disappearance of the isocyanate peak at 2260 cm^{-1} and thiol peak at 2560 cm^{-1}, respectively. After reaction, the solvent was removed by a rotary evaporator and the product was obtained for the next step.

General procedure for the preparation of thiourethane bridged polysilsesquioxane aerogels

The three kinds of thiourethane bridged polysilsesquioxane aerogels are designated as SH-NCO-A, SH-NCO-B and SH-NCO-C, corresponding to the precursors HDI-BSQ, H_{12}MDI-BSQ and MDI-BSQ, respectively. The subsequent number characterizes the precursor reaction concentration. For example, "SH-NCO-A-0.107" means the precursor is HDI-BSQ, and the precursor reaction concentration is 0.107 mol L^{-1}. The general procedure for the preparation of thiourethane bridged polysilsesquioxane aerogel was described below. A certain amount of silsesqiuoxane precursor and ethanol were mixed into a reaction bottle, then hydrochloric acid (0.89 g) was added under stirring at room temperature, and the stirring was continued for 1 min. In the fabrication process, hydrochloric acid was act as catalyst and the final molar ratio of H^+/Si was 3.5. The resultant solution was placed in sealed molds at 60 ºC for 24h to complete gelation and aging. After that the alcogel was transformed from the mold and subjected to solvent exchange with ethanol (6 times in 48 h). After that, the gel was submersed in n-heptane, and the solvent was exchanged six times (in 48 h). Then, the gel was dried by vacuum drying method to obtain aerogel. The sample was further dried at 80 ºC for 4 h to make sure of the complete evaporation of pore liquid.

Characterization:

^1H NMR and ^{29}Si NMR measurements were carried out on Bruker AV-400 and AV-600 NMR instrument, respectively, using the deuterated solvents. The condensation degree (CD) can be calculated according to the following equation $CD = (T^1+2T^2+3T^3)/3$, where T^i refers to the $R{-}Si(OSi)_i(OR')_{3-i}$ species (R' = H or Me). Fourier Transformation Infrared (FTIR) spectrum was obtained using NICOLET-AVATAR-330 spectrometer. The surface microstructure was examined by Scanning Electron Microscope (SEM) (6700F) instrument. Contact angle data was obtained on Krüss Drop Shape Analysis System-100 (DSA 100) by a sessile water drop method with 5 μL liquid drop. Thermogravimetric analysis (TGA) was made using a 7 Series thermal analysis system (Perkin-Elmer). The specimen was heated from 30 to 800 °C at a rate of 10 °C min^{-1} in a dynamic nitrogen atmosphere with a flow rate of 70 mL min^{-1}. Bulk density was obtained from the weight/volume ratio of specimen. The skeletal density was measured by UltraPYC 1200e automatic density analyzer from Quantachrome Instruments. The porosity (Φ) of each specimen was calculated as $(1-\rho_b/\rho_s) \times 100\%$, where ρ_b and ρ_s refers to the bulk and skeletal density, respectively. Specific surface area and pore size was determined by ASAP 2020 specific surface area and porosity analyzer. Adsorption/desorption isotherm was collected by using nitrogen as the adsorbent at 77 K using liquid nitrogen bath to achieve this temperature. The specific surface area and pore size was calculated by the BET (Brunauer–Emmett–Teller) method and BJH (Barrett–Joyner–Halenda) method, respectively. Mechanical property of specimen was measured by compression experiments using a WDT-10INSTRON 3365 tensile tester with a strain rate of 1 mm min^{-1}. The effective thermal conductivity of the specimen was measured by 3ω method using a very thin Pt wire as sensor. When measured, the cylindrical aerogel was cut into two pieces through the axis by using sharp thin blade to ensure the section is very flat and smooth. The Pt wire which diameter is about 19μm is soldered on two thin Cu pillars, which diameter is about 0.5mm. A support was designed to ensure that the two sections can be closely contact with each other when the sensor is sandwiched between them. Furthermore, the support can make sure that the clamping force of the support will not lead to excessive deformation of the aerogels.

Chemical structures characterization of thiourethane bridged silsesquioxane precursors

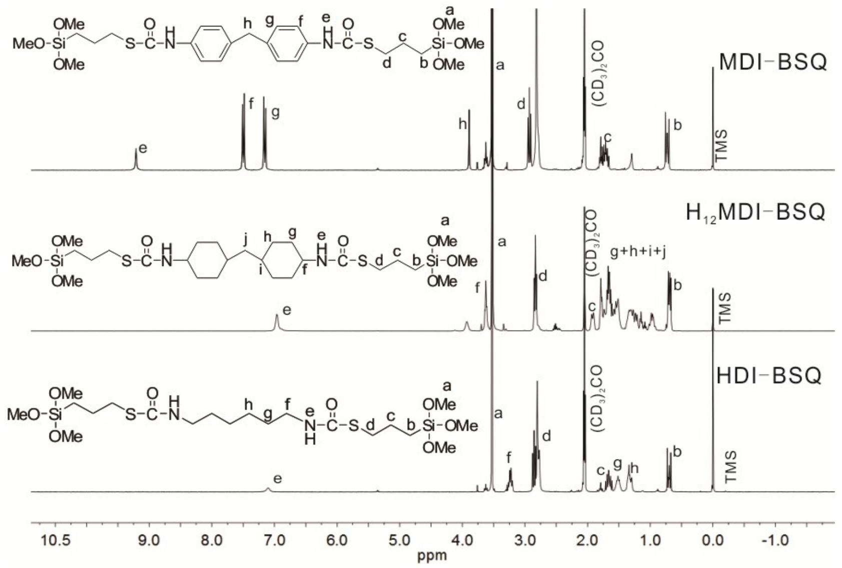

Fig. S1 ^{1}H NMR spectra of HDI-BSQ, H$_{12}$MDI-BSQ and MDI-BSQ.

For HDI-BSQ, ^{1}H NMR (400 MHz, $\mathrm{(CD_3)_2CO}$, δ, ppm) 0.67-0.72 (4H, $\mathrm{-S-(CH_2CH_2C\underline{H_2})-Si-}$), 1.3-1.4 (4H, $\mathrm{-(CH_2CH_2C\underline{H_2}C\underline{H_2}CH_2CH_2)-}$), 1.49-1.54 (4H, $\mathrm{-(CH_2C\underline{H_2}CH_2CH_2C\underline{H_2}CH_2)-}$), 1.61-1.71 (4H,$\mathrm{-S-(CH_2C\underline{H_2}CH_2)-Si-}$),2.77-2.83(4H,$\mathrm{-S-(C\underline{H_2}CH_2CH_2)-Si-}$),3.20-3.29(4H,$\mathrm{-(C\underline{H_2}CH_2CH_2CH_2CH_2C\underline{H_2})-}$), 3.5 (18H, $\mathrm{Si-(OC\underline{H_3})_3}$), 7.1 (2H, $\mathrm{-N\underline{H}-}$);

For H$_{12}$MDI-BSQ, ^{1}H NMR (400 MHz, $\mathrm{(CD_3)_2CO}$, δ, ppm) 0.67-0.72 (4H, $\mathrm{-S-(CH_2CH_2C\underline{H_2})-Si-}$), 0.95-1.79 (20H, $\mathrm{-(C\underline{H_2}C\underline{H}(C\underline{H_2})_2(C\underline{H_2})_2CH)NH-}$), 1.61-1.71 (4H, $\mathrm{-S-(CH_2C\underline{H_2}CH_2)-Si-}$), 2.80-2.86 (4H, $\mathrm{-S-(C\underline{H_2}CH_2CH_2)-Si-}$), 3.5 (18H, $\mathrm{Si-(OC\underline{H_3})_3}$), 3.9 (2H, $\mathrm{-C\underline{H}-NH-CO-}$);6.96 (2H, $\mathrm{-N\underline{H}-}$);

For MDI-BSQ, ^{1}H NMR (400 MHz, $\mathrm{(CD_3)_2CO}$, δ, ppm) 0.67-0.72 (4H, $\mathrm{-S-(CH_2CH_2C\underline{H_2})-Si-}$), 1.66-1.81 (4H, $\mathrm{-S-(CH_2C\underline{H_2}CH_2)-Si-}$), 2.86-2.95 (4H, $\mathrm{-S-(C\underline{H_2}CH_2CH_2)-Si-}$), 3.5 (18H, $\mathrm{Si-(OC\underline{H_3})_3}$), 3.89 (2H, $\mathrm{-Ph-C\underline{H_2}-Ph-}$);7.14-7.17 (4H, $\mathrm{-CH_2-C-C\underline{H}-CH\ -C-NH-}$),7.48-7.51 (4H, $\mathrm{-CH_2-C-CH-C\underline{H}\ -C-NH-}$), 9.2 (2H, $\mathrm{-N\underline{H}-}$)

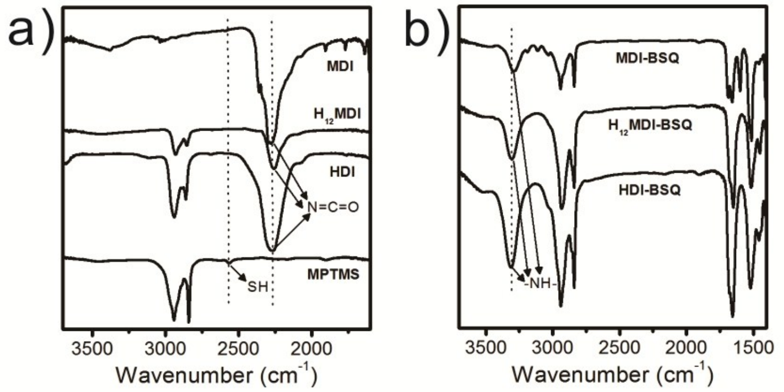

Fig. S2 (a) FTIR spectra of MPTMS, HDI, H$_{12}$MDI and MDI. (b) FTIR spectra of HDI-BSQ, H$_{12}$MDI-BSQ and MDI-BSQ.

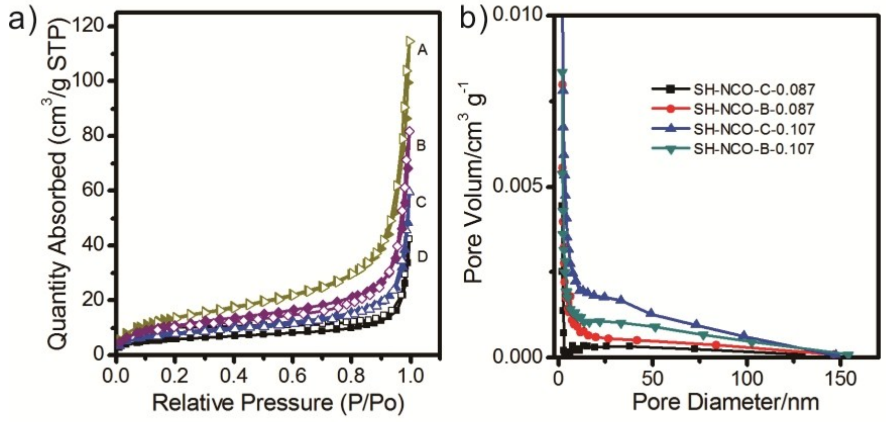

Fig. S3 (a) N_2-sorption data of thiourethane brigded silsesquioxane aerogels: (A) SH-NCO-C-0.107, (B) SH-NCO-B-0.107, (C) SH-NCO-B-0.087, (D) SH-NCO-C-0.087. (b) Pore size distributions of the thiourethane brigded silsesquioxane aerogels.

Table S1 Physical property comparison of thiourethane brigded silsesquioxane aerogels with previous works

Materials	ρ (g cm^{-3})	Φ (%)	S_{BET} (m^2 g^{-1})	E (MPa)	References
Thiourethane PSQ aerogels	0.059	95.3	30.1	0.076	This work
Silica aerogels	0.123	94.41	649	0.209	[1]
Bridged Silsesquioxane aerogels	0.125±0.002	92.0±0.1	58.8±0.04	0.11±0.02	[2]
1,4-phenylene-bridged Polysilsesquioxane aerogels	0.27	-	962	-	[3]
Hexylene -bridged polysilsesquioxane aerogels	0.093±0.003	-	778±40	0.079+0.018	[4]
Xerogels/silica nanoparticles	0.218	-	34±2	10±3	[5]

ρ : the bulk density of the sample, Φ: the porosity of the sample, "-" : the properties not be discussed in the reference, S_{BET} : the specific surface area of the sample, E: the Young's modulus.

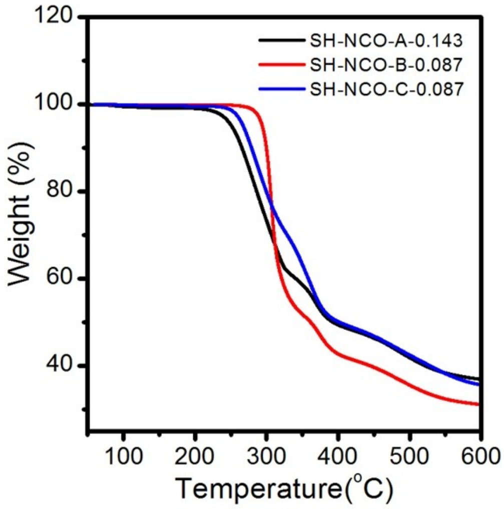

Fig. S3 Representative Thermogravimetric analysis data of aerogels.

In theory, the total thermal conductivity (λ_{total}) of the aerogel in air should contain three components:

the thermal conductivities of by solid phase (λ_s), gas phase (λ_g), and radiation (λ_r):

$$\lambda_{total} = \lambda_s + \lambda_g + \lambda_r$$

The thermal conductivity by radiation is relatively small in the most applications and it can be ignored, so the thermal conductivity of aerogel is mainly derived from λ_s and λ_g. As reported, the thermal conductivities of solid phase and gas phase can be significantly reduced by decreasing the density and narrowing the pore size.

Table S2 Thermal conductivity comparison of the thiourethane bridged polysilsesquioxane aerogel with other thermal insulation materials

Materials	Density (g cm^{-3})	Thermal conductivity (W m^{-1} K^{-1})	References
SH-NCO-B-0.087	0.059	0.019	This work
silica aerogels	0.45	0.015	[6]
bridged silsesquioxane aerogels	0.125	0.037	[2]
Polyurethane aerogels	0.375	0.036	[7]
Polyurethane foam	0.080-0.120	0.039-0.043	[8]
Alumina aerogels	0.135	0.031	[9]

As show in Table 2, the thermal conductivity of SH-NCO-A aerogels decrease from 0.021 W m^{-1} K^{-1} to 0.019 W m^{-1} K^{-1} when the reaction concentration increase from 0.107 mol L^{-1} to 0.143 mol L^{-1}, the decrease of the thermal conductivity is caused by the decrease of the pore size. However, the thermal conductivity of SH-NCO-A aerogels is not decrease but increase to 0.020 W m^{-1} K^{-1} when the reaction concentration increase to 0.155 mol L^{-1}. That is due to the increase of density of the aerogels. On the other hand, the thermal conductivity of PSQ aerogels decrease when the rigidity of bridging group increase, for example, when the reaction concentration is 0.107 mol L^{-1}, the thermal conductivities of SH-CNO-A and SH-NCO-C are 0.021 W m^{-1} K^{-1} and 0.018 W m^{-1} K^{-1}, respectively. That is because, the more rigid bridging groups the silsesquioxane precursors own, the smaller pore size and finer nanostructures the corresponding final aerogels have. The PSQ aerogels own low densities and their pore sizes (Table 1) are smaller than the value of the mean free path of the molecules in air (ca. 70nm), so the λ_s and λ_g of these aerogels will be significant reduced and endow the aerogels low thermal conductivity.

References

1. A. Dourbash, S. Motahari and H. Omranpour, *J. Non-Cryst. Solids*, 2014, **405**, 135-140.
2. S. Yun, H. Luo and Y. Gao, *J. Mater. Chem. A*, 2015, **3**, 3390-3398.
3. D. W. Schaefer, G. Beaucage, D. A. Loy and K. J. Shea, *Chem. Mater.*, 2004, **16**, 1402-1410.
4. D. J. Boday, R. J. Stover, B. Muriithi and D. A. Loy, *J. Sol-Gel Sci. Technol.*, 2011, **61**, 144-150.
5. M. Börner, T. Noisser and G. Reichenauer, *Chem. Mater.*, 2013, **25**, 3648-3653.
6. G. Hayase, K. Kugimiya, M. Ogawa, Y. Kodera, K. Kanamori and K. Nakanishi, *J. Mater. Chem. A*, 2014, **2**, 6525-6531.
7. C. Chidambareswarapattar, P. M. McCarver, H. Luo, H. Lu, C. Sotiriou-Leventis and N. Leventis, *Chem. Mater.*, 2013, **25**, 3205-3224.
8. N. V. Gama, B. Soares, C. S. R. Freire, R. Silva, C. P. Neto, A. Barros-Timmons and A. Ferreira, *Mater. Des.*, 2015, **76**, 77-85.
9. G. Zu, J. Shen, L. Zou, W. Wang, Y. Lian, Z. Zhang and A. Du, *Chem. Mater.*, 2013, **25**, 4757-4764.